Modified Constrained Notch Fourier Transform (MCNFT) for Sinusoidal Signals in Noise and Its Performance

Yegui Xiao

Faculty of Human Life and Environmental Science
Hiroshima Prefectural Women's University, Hiroshima, 734-8558 Japan
xiao@hirojo-u.ac.jp

Abstract *Adaptive Fourier analysis of sinusoidal signals in noise is of essential importance in many engineering fields. So far, many adaptive algorithms have been developed for this purpose. In particular, a filter bank based algorithm called constrained notch Fourier transform (CNFT) is one of them, which is very attractive in terms of its cost-efficiency and easily controllable performance. However, its performance deteriorates when the signal frequencies are not uniformly spaced.*

This paper proposes, at first, a new structure for the CNFT, referred to as modified CNFT (MCNFT), to compensate the performance degeneration of the CNFT for noisy sinusoidal signals with non-uniformly spaced frequencies. Next, a detailed performance analysis for the MCNFT is conducted. Closed form expression of steady-state mean square error (MSE) for the discrete Fourier coefficients (DFCs) is derived. Extensive simulations are presented to demonstrate the improved performance of the MCNFT and the validity of the analytical results.

1 Introduction

Adaptive estimation of sinusoidal signals or quasi-periodic signals is a very important topic in many engineering fields, such as digital communications, power systems, control, sonar, biomedical engineering and pitch detection in automated transcription, just to name a few. Generally, the well-known DFT and short-time DFT are simple and cost-efficient tools for these applications. They are awkward, however, when the signals of interest are nonstationary and/or the frequencies of interest are arbitrary or not the integer multiple of the fundamental frequency.

To combat the above-mentioned difficulties with the DFT, a number of adaptive techniques have been developed. The Kalman filtering based techniques [1,2], the recursive least square (RLS) algorithm [3], the simplified RLS (SRLS) algorithm [4,5], the LMS [6,7, and references therein], the least mean p-power error criterion based algorithm [8] are some of them. In particular, the filter bank based techniques, the Fourier notch transform (NFT) by Tadokoro, et al. [9] and the constrained NFT (CNFT) by Kilani et al. [10], are quite attractive due to their cost efficiencies and reasonable performances. The steady-state performances of the NFT and the CNFT for signals with uniformly spaced frequencies have been conducted in [11] in detail. The NFT is very simple in structure but generally not robust to additive noise. The CNFT is more robust than the NFT but its performance degenerates severely when the signal frequencies are arbitrarily spaced.

In this paper, we first propose a new structure for the CNFT, referred to as modified CNFT (MCNFT), to compensate the performance degeneration of the CNFT for sinusoidal signals with non-uniformly spaced frequencies. Next, we will conduct a detailed performance analysis for the MCNFT, deriving steady-state mean square error (MSE) of the discrete Fourier coefficient (DFC) estimates. Extensive simulations will be performed to demonstrate the improved performance of the MCNFT and the validity of the analytical findings as well.

The rest of this paper is organized as follows. Section 2 presents the MCNFT. The performance analysis of the MCNFT is given in Section 3. Simulation results are shown in Sections 2 and 3 whenever needed. Section 4 concludes the paper briefly.

2 The MCNFT

Consider a sinusoidal signal in noise

$$x(n) = \sum_{i=1}^{Q} (a_i \cos \omega_i n + b_i \sin \omega_i n) + v(n) \qquad (1)$$

where n denotes the discrete time instant. ω_i's ($i = 1, 2, \cdots, Q$) are arbitrary signal frequencies that are not uniformly spaced. Q is the number of frequency components contained in the signal. $v(n)$ is an additive white Gaussian noise with zero mean and variance σ_v^2. The CNFT used to adaptively estimate the DFCs, a_i and b_i, is depicted in Fig.1, where

$$\begin{aligned} H_{BP,i}(z) &= (\rho - 1)\frac{\kappa_i z^{-1} + (\rho + 1) z^{-2}}{1 + \kappa_i \rho z^{-1} + \rho^2 z^{-2}}, \qquad (2) \\ \kappa_i &= -2 \cos \omega_i. \end{aligned}$$

In Fig.1, the steady-state output of the i-th channel is

$$y_i(n) = a_i \cos \omega_i n + b_i \sin \omega_i n + v_i \qquad (3)$$

where v_i is an additive noise signal at the i-th channel output due to the additive noise $v(t)$ residing in the input signal $x(n)$. The variance of this zero-mean noise can be calculated using the theory of residues, as follows (see Appendix for details)

$$\sigma_{v_i}^2 = \{\frac{2(1-\rho)}{1+\rho} - \frac{2(1-\rho)^2}{1+\rho}\frac{\rho^2+\rho-2}{\rho^4-2\rho^2\cos 2\omega_i+1} - \frac{(1-\rho)^3}{1+\rho}\frac{(1+\rho)^2+4\sin^2\omega_i}{\rho^4-2\rho^2\cos 2\omega_i+1}\}\sigma_v^2. \quad (4)$$

Clearly, the noise $v_i(n)$ will be largely depressed by the bandpass filter, and sinusoids with less noise will be available at the output of each channel, if the pole radius is close to unit.

The sliding algorithm of the CNFT is given by

$$\hat{a}_i(n) = \frac{1}{\sin\omega_i}\{y_i(n-1)\sin\omega_i n - y_i(n)\sin\omega_i(n-1)\}, \quad (5)$$

$$\hat{b}_i(n) = \frac{1}{\sin\omega_i}\{-y_i(n-1)\cos\omega_i n + y_i(n)\cos\omega_i(n-1)\}. \quad (6)$$

However, the DFCs estimates generated by the above algorithm have been found to contain sinusoidal fluctuations at steady-state due to the leakage of frequency components through the bandpass filters. This implies a performance degeneration. A new structure is proposed in Fig. 2 to modify the CNFT to remove the fluctuations within the DFCs estimates, where

$$y_i(n|n-1) = \hat{a}_i(n-1)\cos\omega_i n + \hat{b}_i(n-1)\sin\omega_i n. \quad (7)$$

The MCNFT also uses the above sliding algorithm to perform the DFCs estimation. Fig. 3 shows a comparison between the DFC estimates of the CNFT and the MCNFT. Clearly, the fluctuations with the CNFT disappear completely with the MCNFT.

3 Performance of the MCNFT

In this section, we assess analytically the steady-state performance of the MCNFT. First the estimation error and then the estimation MSE will be investigated and their closed form expressions will be derived. We also provide some typical simulation results to validate the analytical expressions obtained.

A: Estimation error

Using (3) in (5) leads to

$$\hat{a}_i(n) = a_i + \frac{1}{\sin\omega_i}\{v_i(n-1)\sin\omega_i n - v_i(n)\sin\omega_i(n-1)\}, \quad (8)$$

$$\hat{b}_i(n) = b_i + \frac{1}{\sin\omega_i}\{-v_i(n-1)\cos\omega_i n + v_i(n)\cos\omega_i(n-1)\}. \quad (9)$$

Obviously, one gets easily from (8) and (9)

$$E[\hat{a}_i(n)-a_i] = 0, \quad E[\hat{b}_i(n)-b_i] = 0, \quad (10)$$

which means that the MCNFT is unbiased. We have found that the NFT and the CNFT are all unbised [11]. Therefore, the proposed MCNFT also shares the same property the CNFT possesses in the mean sense.

B: Estimation MSE

From (8), the MSE of the cosine DFC can be derived as below.

$$V_{a_i} = E[(\hat{a}_i(n)-a_i)^2] = \frac{1}{\sin^2\omega_i}\sigma_{v_i}^2 - \frac{\cos\omega_i}{\sin^2\omega_i}E[v_i(n)v_i(n-1)] \quad (11)$$

Furthermore, it can be easily found that the MSE of the sine DFC is the same as the MSE of the cosine DFC.

$$V_{b_i} = E[(\hat{b}_i(n)-b_i)^2] = V_{a_i} \quad (12)$$

The auto-correlation of $v_i(n)$ can be calculated by (see the Appendix for details)

$$E[v_i(n)v_i(n-1)] = \left\{\frac{2(1-\rho)}{1+\rho} - 8\rho(1-\rho)^2\frac{\sin^2\omega_i}{\rho^4-2\rho^2\cos 2\omega_i+1} + \frac{2(1-\rho)^3}{1+\rho}\frac{\rho^3+2\rho^2-2}{\rho^4-2\rho^2\cos 2\omega_i+1}\right\}\sigma_v^2\cos\omega_i \quad (13)$$

Consequently, using (13) and (4) in (11), the MSE may be ultimately expressed by

$$V_{a_i} = \left[\frac{2(1-\rho)}{1+\rho} + \frac{2(1-\rho)^2\{2-\rho(\rho+1)\cos^2 2\omega_i\}}{(1+\rho)(\rho^4-2\rho^2\cos 2\omega_i+1)\sin^2\omega_i} - \frac{(1-\rho)^3\{\rho^2+2\rho+5+2(\rho^3+2\rho^2-4)\cos^2\omega_i\}}{(1+\rho)(\rho^4-2\rho^2\cos 2\omega_i+1)\sin^2\omega_i}\right]\sigma_v^2 \quad (14)$$

Here, we have the following comments in order

1. The MSE is proportional to the variance of the additive noise, which is a common property for many adaptive algorithms.
2. It can be seen that the narrower the notch bandwidth, i.e. the closer the pole radius ρ to unit, the smaller the MSE will be.
3. The MSE depends on not only the variance of the additive noise and the pole radius but also on the signal frequency. This property can not be predicted before the analysis is done. It is also clear that the dependence of the MSE on the signal frequency will become neglectable as the pole radius approaches unit, since the 2nd and 3rd terms of the RHS of (14) gets much smaller compared to the 1st term.

Here, we provide two simulation results in Figs. 4 and 5 to peek at the validity of the analytical expression for the steady-state MSE. We see from Figs. 4 and 5 that the theory follows the simulated points excellently. It may also be noted that the steady-state MSE gets smaller in almost a linear fashion as ρ approaches unit, and becomes larger for small and large signal frequencies.

4 Conclusions

A modified CNFT (MCNFT) structure has been proposed and its steady-state performance has also been assessed analytically. Simulations have been performed to see the improved performance of the MCNFT and the accuracy of the analytical expressions. Tracking analysis of the CNFT and the MCNFT is left for further research.

Acknowledgments

A part of the simulations in this work was performed by Mr. T. Matsuo, Saga University, and is appreciated. Thanks are also given to Prof. K. Shida, Dr. A. Kimoto, and Mr. H. Yoshida, Saga University, for their helpful discussions.

Appendix

A: Calculation of $\sigma_{v_i}^2$

First, one has

$$\sigma_{v_i}^2 = \frac{\sigma_v^2}{2\pi j}\oint_C H_{BP,i}(z)H_{BP,i}(z^{-1})\frac{dz}{z} \tag{15}$$

where C is a unit circle centered at the origin in the z-domain. Using (2) in the above equation leads to

$$\sigma_{v_i}^2 = \frac{\sigma_v^2}{2\pi j}(\rho-1)^2\oint_C \frac{\kappa_i z+(\rho+1)}{z^2+\rho\kappa_i z+\rho^2}\frac{\kappa_i+(\rho+1)z}{1+\rho\kappa_i z+\rho^2 z^2}dz \tag{16}$$

Using the theory of residues, one gets

$$\begin{aligned}\sigma_{v_i}^2 &= Res(\rho e^{j\omega_i}) + Res(\rho e^{-j\omega_i}) \\ &= \frac{1-\rho}{(1+\rho)(\rho^4-2\rho^2\cos 2\omega_i+1)} \\ &\quad\times\{\kappa_i^2+4\kappa_i\rho(\rho+1)\cos\omega_i+(\rho+1)^2 \\ &\quad+\kappa_i^2\rho^2+\rho^2(\rho+1)^2\}\sigma_v^2\end{aligned} \tag{17}$$

Putting κ_i into (17) yields (4) readily.

B: Calculation of $E[v_i(n)v_i(n-1)]$

Let $h_i(k)$, $k=0,1,\cdots,\infty$ be impulse response of the i-th bandpass filter $H_{BP,k}(z)$. One has

$$\begin{aligned}E[v_i(n)v_i(n-1)] &= \sum_{k=0}^{\infty}h_i(k)v_i(n-k) \\ &\quad\times\sum_{m=0}^{\infty}h_i(m)v_i(n-1-m) \\ &= \sum_{k=0}^{\infty}h_i(k)h_i(k-1)\sigma_v^2\end{aligned} \tag{18}$$

and

$$\sum_{k=0}^{\infty}h_i(k)h_i(k-1) = \frac{1}{2\pi j}\oint_C H_{BP,i}(\nu)H_{BP,i}(\frac{1}{\nu})d\nu. \tag{19}$$

Using the theory of residues, we have

$$\begin{aligned}Res(\rho e^{j\omega_i}) &= \frac{(1-\rho)^2}{1-\rho^2}\frac{\kappa_i\rho e^{j\omega_i}+(\rho+1)}{\rho(e^{j\omega_i}-e^{-j\omega_i})} \\ &\quad\times\frac{\kappa_i\rho e^{j\omega_i}+(\rho+1)\rho^2e^{j2\omega_i}}{1-\rho^2e^{j2\omega_i}}\end{aligned} \tag{20}$$

$$\begin{aligned}Res(\rho e^{-j\omega_i}) &= \frac{(1-\rho)^2}{1-\rho^2}\frac{\kappa_i\rho e^{-j\omega_i}+(\rho+1)}{\rho(e^{-j\omega_i}-e^{j\omega_i})} \\ &\quad\times\frac{\kappa_i\rho e^{-j\omega_i}+(\rho+1)\rho^2e^{-j2\omega_i}}{1-\rho^2e^{-j2\omega_i}}\end{aligned} \tag{21}$$

and finally,

$$\begin{aligned}&E[v_i(n)v_i(n-1)] \\ &= Res(\rho e^{j\omega_i}) + Res(\rho e^{-j\omega_i}) \\ &= (13).\end{aligned} \tag{22}$$

References

[1] R. R. Bitmead, A. C. Tsoi and P. J. Parker, *"A Kalman filtering approach to short-term Fourier analysis,"* IEEE Trans. Acoust., Speech, Signal Processing, Vol.ASSP-34, No.6, pp.1493-1501(1986).

[2] P. Gruber and J. Todtli, *"Estimation of quasi-periodic signal parameters by means of dynamic signal models,"* IEEE Trans. Signal Processing, Vol.42, No.3, pp.552-562(1994).

[3] N. K. M'sirdi et al., *"An RML algorithm for retrieval of sinusoids with cascaded notch filters,"* ICASSP-1988, pp.2484-2487(1988).

[4] S. Pei and C. Tseng, *"Real time cascade adaptive notch filter scheme for sinusoidal parameter estimation,"* Signal Processing, Vol.39, pp.117-130(1994).

[5] Y. Xiao, Y. Tadokoro, K. Shida, and K. Iwamoto, *"Performance analysis of a simplified RLS algorithm for the estimation of sinusoidal signal in additive noise,"* IEICE Trans on Fundamentals,Vol.E81-A, No.8, pp.1703-1712(1998).

[6] C. A. Vaz and N. V. Thakor, *"Adaptive Fourier estimation of time-varying evoked potentials,"* IEEE Trans. Biomed. Eng., Vol.36, pp.448-455(1989).

[7] Y. Xiao, Y. Tadokoro, and K. Iwamoto, *"Real-valued LMS Fourier analyzer for sinusoidal signals in noise,"* Signal Processing, 69, pp.131-147(1998).

[8] Y. Xiao, Y. Tadokoro, and K. Shida, *"Adaptive algorithm based on least mean p-power error criterion for Fourier analysis in additive noise,"* IEEE Trans. on Signal Processing, Vol.47, No.4, pp.1172-1181(1999).

[9] Y. Tadokoro and K. Abe, *"Notch Fourier transform,"* IEEE Trans. Acoust., Speech, Signal Processing, Vol.ASSP-35, No.9, pp.1282-1288(1987).

[10] M. T. Kilani and J. F. Chicharo, *"A constrained notch Fourier transform,"* IEEE Trans. on Signal Processing, Vol.43, No.9, pp.2058-2067(1995).

[11] Y. Xiao, T. Matsuo, and K. Shida, *"Performance analysis of notch Fourier transform (NFT) and constrained notch Fourier transform (CNFT),"* IEICE Trans. on Fundmentals, (Accepted for publication, 2000).

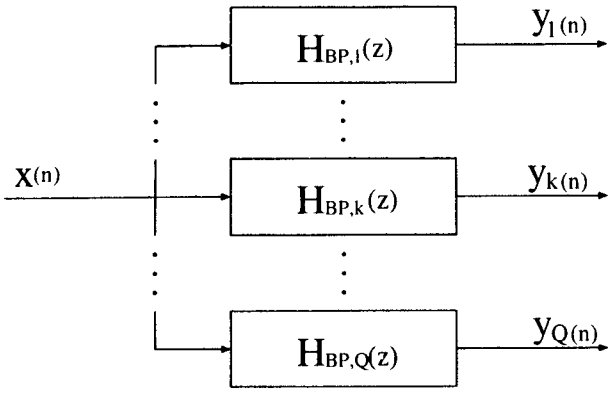

Fig.1 Filter bank implementation for the CNFT for sinusoidal signals with arbitrarily distributed frequencies.

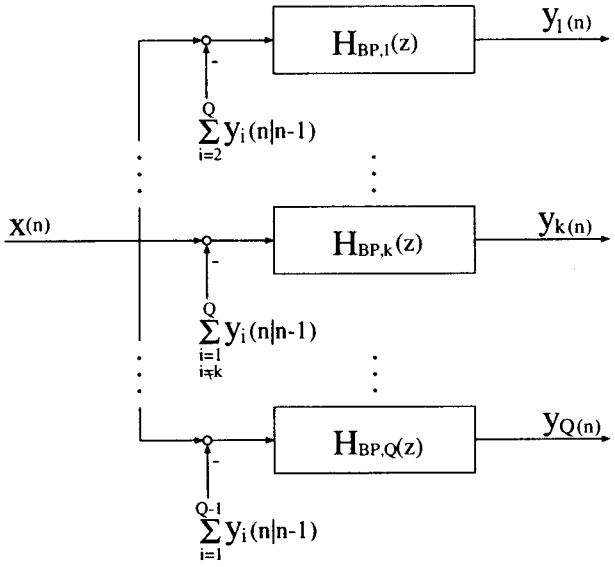

Fig.2 Filter bank implementation for the MCNFT for sinusoidal signals with arbitrarily distributed frequencies.

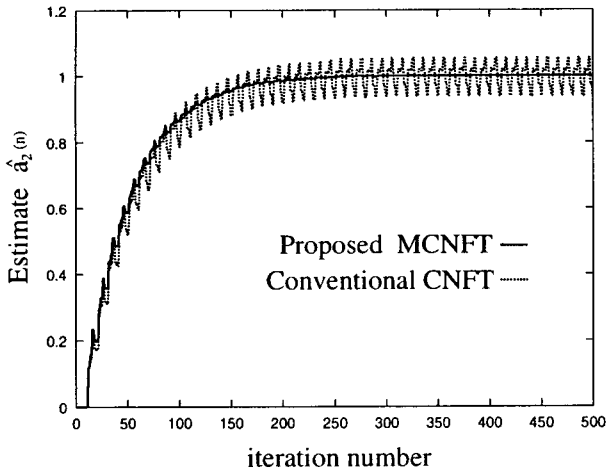

(a) DFC estimates

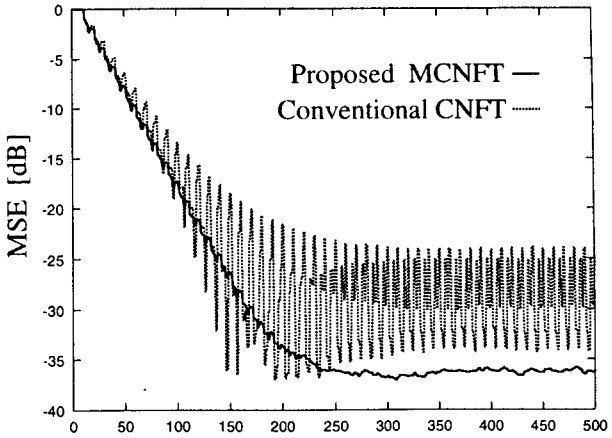

(b) MSE

Fig.3 DFCs estimates and MSEs by the CNFT and the MCNFT for sinusoidal signal with non-uniformly spaced frequencies (SNR = 10 [dB], $\rho = 0.9$, $\omega_0 = 0.2\pi$, 100 runs).

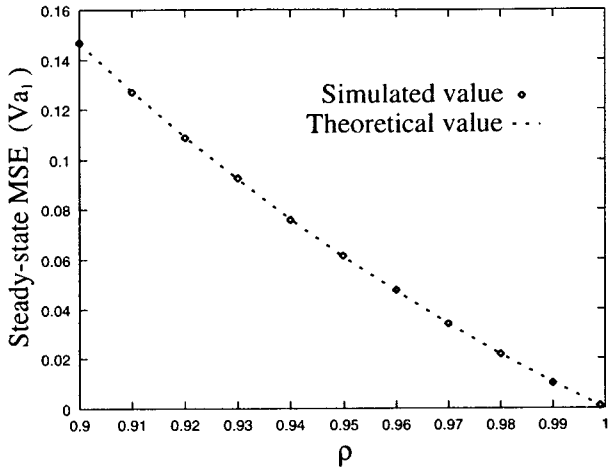

Fig.4 Comparison between theoretical and simulated MSEs of a DFC estimate by the MCNFT versus the pole radius ρ (SNR = 10 [dB], $\omega_0 = 0.2\pi$, 100 runs).

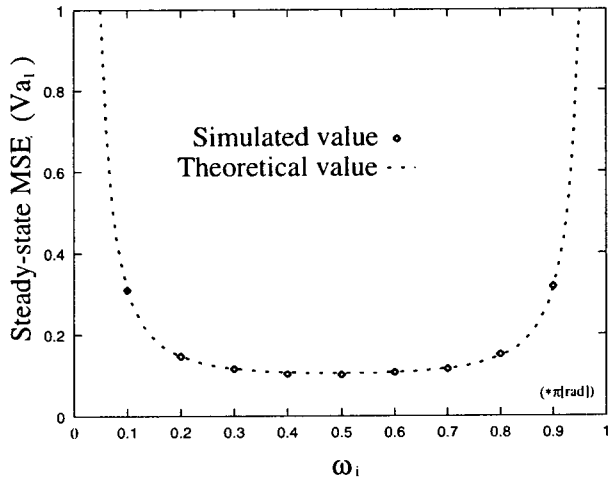

Fig.5 Comparison between theoretical and simulated MSEs of a DFC estimate by the MCNFT versus the signal frequency (SNR = 10 [dB], $\rho = 0.9$, $\omega_0 = 0.2\pi$, 100 runs).